

Colloidal PbS Quantum Dot Photodetectors for Short-wave Infrared applications

Chen Hu,^{1,2,3} Alban Gassenq,^{1,2} Eva M.P. Ryckeboer,^{1,2} Yolanda Justo,^{2,3} Zeger Hens,^{2,3} and Gunther Roelkens^{1,2}

¹ Photonics Research Group, INTEC Department, Ghent University-IMEC, Sint-Pietersnieuwstraat 41, 9000 Ghent, Belgium

² Center for Nano- and Biophotonics (NB-Photonics), Ghent University, Belgium

³ Physics and Chemistry of Nanostructures, Ghent University, Krijgslaan 281-S3, 9000 Gent, Belgium

In this study, the use of PbS colloidal quantum dots for short-wave infrared photodetector applications is explored. To achieve effective carrier transport between the dots in a film, a layer-by-layer approach is used to deposit uniform, ultra-smooth and crack-free QD films, where each deposition cycle involves the replacement of the native organic ligands by inorganic moieties (OH⁻ and S²⁻) followed by a thorough cleaning procedure. The photodetector shows clear photoconductive gain. The cut-off wavelength of these devices is ~ 2.2 μm. Integration of these photodetectors on silicon photonic circuits is demonstrated.

Introduction

Nowadays the short-wave infrared (SWIR) region gets more and more attention for applications. Traditional spectroscopic systems are nowadays mainly based on discrete components based on epitaxial materials¹. However, the cost of these components hampers large scale deployment of such systems and the size of the system makes their use difficult in the field. Low cost colloidal quantum dots (QDs) offer an alternative way to implement SWIR photodetectors and can be integrated on silicon-based waveguide circuits, resulting in very small and cheap spectroscopic sensing systems². Colloidal QDs are new optoelectronic materials that raise a lot of interest for photonic applications. They are prepared by simple hot injection chemical synthesis, which offers a significant cost reduction³. Another advantage of colloidal QDs is the spectral tunability due to the quantum size effect⁴. The suspension of colloidal QDs in solution provides an easy way to realize large-area heterogeneous integration by solution based processing⁵.

In this study we use PbS colloidal QDs for short-wave infrared photodetector applications. A layer-by-layer (LBL) approach is demonstrated to realize homogeneous and crack-free QD films. In this approach, each cycle involves a QD layer deposition by dip coating, followed by inorganic ligand exchange, and then a thorough cleaning procedure is used to remove impurities. Metal-free inorganic ligands, such as OH⁻ and S²⁻, are used to enhance carrier transport in QD films⁶. The QD films are realized on prefabricated interdigitated electrodes (for surface illuminated devices) and also on silicon photonics planar concave grating spectrometers (PCG). Afterwards a selective wet etching approach is used to achieve a micropatterned QD film.

Experimental details

1. Fabrication of QD films

The QD films were formed by a layer-by-layer (LBL) approach. Each cycle contains a dip coating of the substrates into a 1 μM PbS QD suspension in toluene with an 80 mm/min dipping speed. After completely drying, the QD films were re-immersed into a solution of either $\text{Na}_2\text{S}\cdot 9\text{H}_2\text{O}$ (10 mg/mL) or KOH (0.01 mg/mL) in formamide to exchange the original oleate ligands by S^{2-} and OH^- . At the end of each cycle, the sample was thoroughly cleaned by immersing it twice in formamide, twice in acetone and once in isopropanol. Afterwards the sample was dried under nitrogen.

2. Micropatterning of QD films

Micropatterned QD films were realized by optical lithography and wet etching. The photoresist was spun on top of the QD layer and post baked. After exposure and development, the pattern was transferred from the mask to the photoresist layer. After this a mixture of HCl and H_3PO_4 was used to remove the uncovered QD film. The volume ratio between HCl and H_3PO_4 is $\sim 1:10$. After the desired etching time, the photoresist was stripped by acetone, resulting in a well defined micropatterned QD film.

3. Photodetector Fabrication

PbS photodetectors are fabricated similar to the PbS thin films. For the surface illuminated PbS photodetectors, an isolating SiO_2 layer was deposited by plasma enhanced chemical vapor deposition (PECVD) on a silicon substrate. A pair of interdigitated finger shape electrodes was formed by optical lithography through a lift-off process consisting of 10 nm Ti and 100 nm Au. The fingers are designed with 2 μm wide fingers with 2 μm separation and are attached to two independent contact pads (shown in Figure 1). For integrated photodetectors on planar concave gratings, an array of electrodes was defined by photolithography and lift-off. After the QD films were deposited with a layer-by-layer (LBL) approach, selective wet etching was used to obtain micropatterned QD detectors for surface illumination on silicon substrate and on photonic integrated circuits.

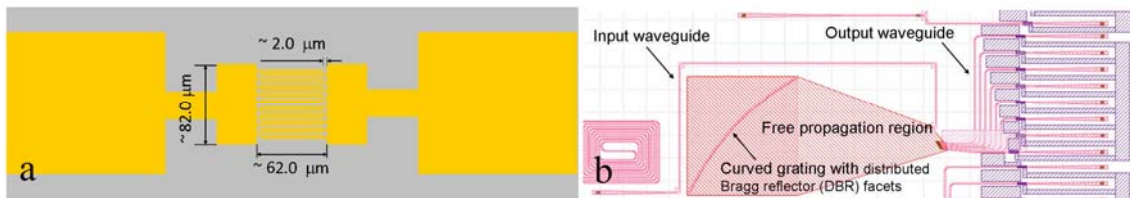


Figure 1. (a) Illustration of the PbS detector electrodes design (top view) (b) schematic of integrated photodetector electrodes design on a planar concave grating

Results and Discussion

1. Layer-by-layer assembly of QD films

After synthesis, the electrically isolating organic oleate ligands need to be replaced by inorganic ligands to facilitate carrier transport in QD films and implement photoconductive devices. Thus a solid state ligand exchange process is proposed to remove the original organic capping of the QDs. Transmission electron microscopy (TEM) is used to examine the ligand exchange of QDs on a small scale. As shown in Figure 2, the distances between QDs are clearly decreased after ligand exchange, which indicates that the oleate ligands were removed after chemical treatment. The corresponding surface morphology of the QD films obtained by the LBL approach is

measured by scanning electron microscopy (SEM), which confirms that crack-free, homogeneous QD films can be obtained.

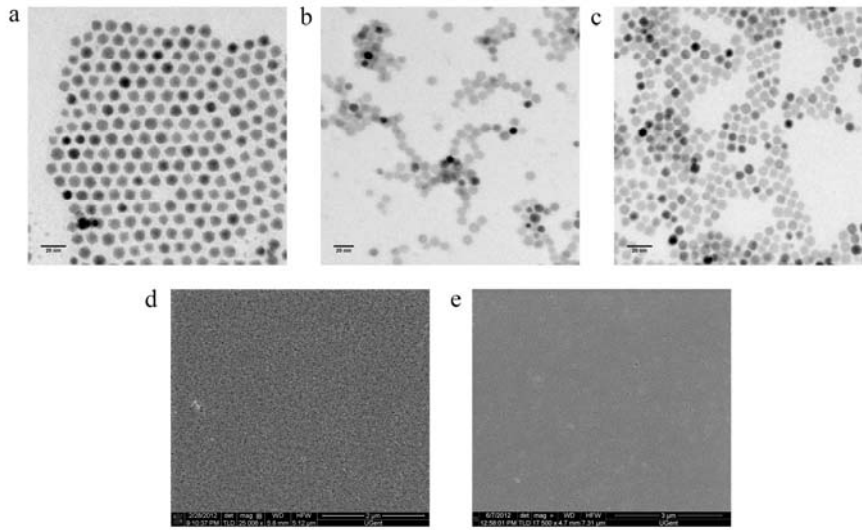


Figure 2. (a) TEM images of OIAc (a), S^{2-} (b) and OH^- (c) -terminated colloidal PbS QDs. SEM images of S^{2-} (d) and OH^- (d) -terminated PbS films.

2. Characterization of PbS photodetectors

The current-voltage characterization of S^{2-} -terminated PbS photodetectors was done under surface illumination with a fiber coupled near infrared SLED ($\lambda \sim 1.55 \mu m$). As shown in Figure 3(b), under illumination, the PbS photodetector shows photoconductive behavior and a linear I-V characteristic is observed, which indicates that the carrier transport is facilitated by the inorganic ligand exchange. The responsivity of S^{2-} -terminated PbS photodetectors as a function of illumination power level is represented in Figure 3(c), which shows an increase of responsivity with decreasing illumination. The photodetector shows internal photoconductive gain, which indicates that the carrier lifetime (related to the trapping of carriers in the dots) is longer than the carrier transit time. Probably, the long-lived trap states are filled with increasing incident power, such that a lower responsivity is obtained for increased input power.

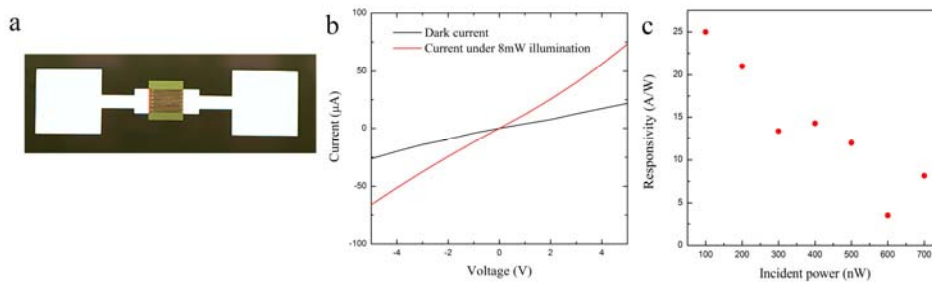


Figure 3. (a) microscope picture of a S^{2-} -terminated PbS colloidal QD photodetector. (b) Current-voltage characteristics of processed S^{2-} -terminated PbS colloidal QD photoconductors. (c) Responsivity dependence as a function of optical power at $1.55 \mu m$ and a bias voltage of 10 V for an S^{2-} -terminated PbS colloidal QD photodetector.

Integrated QD photodetectors are obtained by the deposition of OH^- -terminated PbS QD on a PCG. This is shown in Figure 4. Measurements are currently being carried out to assess the performance of such a spectrometer.

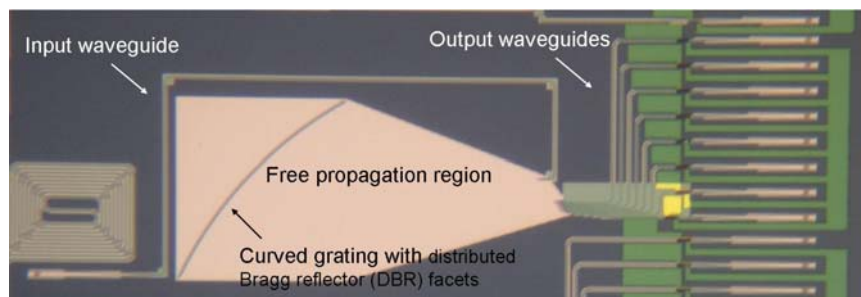


Figure 4. microscope picture of a OH^- -terminated PbS colloidal QD photodetector array integrated on a planar concave grating spectrometer.

Conclusions

In this paper, PbS QDs are explored for SWIR photodetector applications. We have demonstrated a uniform, ultra-smooth colloidal QD film without cracks by the LBL assembly method. Metal-free inorganic ligands, such as OH^- and S^{2-} are investigated to facilitate the charge carrier transport between the dots. PbS photoconductors show clear photoconductive gain. The integration of PbS QD photodetectors on photonic integrated circuits has also been realized.

Acknowledgements

This work is supported by the FWO-NanoMIR project and the FP7-ERC-MIRACLE project. We acknowledge the assistance from Steven Verstuyft during the device fabrication. We also acknowledge the assistance from Liesbet Van Landschoot and Kasia Komorowska during SEM measurement.

References

- [1] Baile Chen, W. Y. Jiang, Jinrong Yuan, Archie L. Holmes, Jr, and Bora. M. Onat, "Demonstration of a room-temperature InP-based photodetector operating beyond $3 \mu\text{m}$ ", *Photonics Technology Letters*, Volume 23, Issue 4, 218–220 (2011).
- [2] Gerasimos Konstantatos, Ian Howard, Armin Fischer, Sjoerd Hoogland, Jason Clifford, Ethan Klem, Larissa Levina & Edward H. Sargent, "Ultrasensitive solution-cast quantum dot photodetectors", *Nature* 442, 180-183 (2006).
- [3] Iwan Moreels, Yolanda Justo, Bram De Geyter, Katrien Haestraete, José C. Martins, and Zeger Hens, "Size-Tunable, Bright, and Stable PbS Quantum Dots: A Surface Chemistry Study", *ACS Nano*, 5 (3), pp 2004–2012 (2011).
- [4] Iwan Moreels, Karel Lambert, Dries Smeets, David De Muynck, Tom Nollet, José C. Martins, Frank Vanhaecke, Andre´ Vantomme, Christophe Delerue, Guy Allan and Zeger Hens, "Size-Dependent Optical Properties of Colloidal PbS Quantum Dots", *ACS Nano* Vol. 3(10), 3023–3030 (2009).
- [5] Michaela Böberl, Maksym V. Kovalenko, Stefan Gamerith, Emil J. W. List, and Wolfgang Heiss, "Inkjet-Printed Nanocrystal Photodetectors Operating up to $3 \mu\text{m}$ Wavelengths", *Adv. Mater.* 19, 3574–3578 (2007).
- [6] Angshuman Nag, Maksym V. Kovalenko, Jong-Soo Lee, Wenyong Liu, Boris Spokoyny, and Dmitri V. Talapin, "Metal-free Inorganic Ligands for Colloidal Nanocrystals: S^{2-} , HS^- , Se^{2-} , HSe^- , Te^{2-} , HTe^- , TeS_3^{2-} , OH^- , and NH_2^- as Surface Ligands", *J. Am. Chem. Soc.* 133, 10612–10620 (2011).